Spatial control of potato tuberisation by the TCP transcription factor BRANCHED1b

Michael Nicolas
Centro Nacional de Biotecnología/CSIC https://orcid.org/0000-0002-7311-5306
Rafael Torres-Perez
Consejo Superior de Investigaciones Científicas https://orcid.org/0000-0002-3696-4720
Vanessa Wahl
Max Planck Institute of Molecular Plant Physiology https://orcid.org/0000-0001-7421-8801
María Luisa Rodríguez-Buey
CNB, CSIC Madrid, Spain
Eduard Cruz-Oró
CNB, CSIC Madrid, Spain
Juan Oliveros
Consejo Superior de Investigaciones Científicas
Salomé Prat
CNB, CSIC Madrid, Spain
Pilar Cubas (pcubas@cnb.csic.es)
Centro Nacional de Biotecnología/CSIC https://orcid.org/0000-0003-4679-2173

Article

Keywords: Solanum tuberosum, tuberisation, bud dormancy, TCP genes, BRANCHED1, sink strength

Posted Date: September 10th, 2020

DOI: https://doi.org/10.21203/rs.3.rs-69596/v1

Version of Record: A version of this preprint was published at Nature Plants on March 21st, 2022. See the published version at https://doi.org/10.1038/s41477-022-01112-2.

Spatial control of potato tuberisation by the TCP transcription factor BRANCHED1b

Michael Nicolas[1,#], Rafael Torres-Perez[2], Vanessa Wahl[3], María Luisa Rodríguez-Buey[1], Eduard Cruz-Oró[1], Juan Carlos Oliveros[2], Salomé Prat[1] and Pilar Cubas[1,#]

1. Plant Molecular Genetics Department, Centro Nacional de Biotecnología-CSIC, Campus Universidad Autónoma de Madrid, 28049, Madrid, Spain
2. Bioinformatics for Genomics and Proteomics Unit, Centro Nacional de Biotecnología-CSIC, Campus Universidad Autónoma de Madrid, Madrid, Spain
3. Department of Metabolic Networks, Max Planck Institute of Molecular Plant Physiology, Am Mühlenberg 1, 14476 Potsdam, Germany.

#Corresponding authors: pcubas@cnb.csic.es, michael.nicolas@cnb.csic.es

Running head: *BRC1b* prevents aerial potato tuberisation

Keywords: *Solanum tuberosum*, tuberisation, bud dormancy, TCP genes, BRANCHED1, sink strength.

Abstract

The control of carbon allocation, storage and usage is critical for plant growth and development and is exploited for both crop food production and CO_2 capture. Potato tubers are natural carbon reserves in the form of starch that have evolved to allow propagation and survival over winter. They form from stolons, below ground, where they are protected from cold temperatures and animal foraging. We show that *BRANCHED1b* (*BRC1b*) acts as a tuberisation repressor in aerial axillary buds, which prevents buds from competing in sink strength with stolons. *BRC1b* loss of function leads to ectopic production of aerial tubers and reduced underground tuberisation. In buds, *BRC1b* promotes dormancy, ABA signalling and downregulation of plasmodesmata gene expression. This limits sucrose unloading and access of the tuberigen factor SP6A to axillary buds. Moreover, BRC1b directly interacts with SP6A and blocks its tuber-forming activity in aerial nodes. Altogether these actions help promote tuberisation underground.

A central question in plant biology is how carbon partitioning is regulated in response to changing environmental conditions, and how this control is integrated with developmental programs. Plant meristems, groups of undifferentiated, actively dividing cells, are sink organs that use sucrose for respiration, growth and development. Under low sucrose availability, they remain quiescent or dormant. Axillary meristems, shoot meristems located in the leaf axils, can give rise to aerial branches with orthotropic growth that produce leaves, inflorescences and flowers. They can also generate stolons, specialised shoots, homologous to branches, that grow horizontally on the soil surface or below ground and have the potential to generate new clonal plants, thus being strategic for vegetative propagation. Branches and stolons differ in their developmental responses to external stimuli, such as day length (see below).

Solanum tuberosum (potato) is one of the best-studied stolon-forming species, as their underground stolons develop energy-rich, starch-accumulating tubers, which constitute a large fraction of the dietary intake for many people worldwide. In the potato landrace ssp. *andigena,* the stolons become strong sinks when winter approaches, and form tubers at their sub-apical region. Tubers overwinter buried in soil, where they are protected from cold and animal foraging, to generate entirely new plants in spring. Tuberisation is controlled by the *FLOWERING LOCUS T (FT)-like SELF-PRUNING 6A* (*SP6A*) gene. In potato ssp. *andigena*, activation of this gene is fully dependent on short days (SD). In long days (LD), the CONSTANS-like1 (COL1) transcription factor represses *SP6A* expression through the activation of another *FT-like* gene, *SP5G*[1,2]. In SD, lack of *SP5G* allows *SP6A* activation, and the SP6A protein is then phloem-transported from leaves to stolons. At the stolon apices, SP6A form a Tuberigen Activation Complex (TAC) that acts to promote tuber formation[3,4].

Unlike stolons, neither branches nor branch primordia, namely axillary buds, undergo tuberisation in SD. The molecular mechanisms that drive these distinct responses

remain unclear. Indeed, in most plant species SD promote shoot bud dormancy, which involves induction of abscisic acid (ABA) signalling and a carbon-starvation syndrome[5–8]. In perennials, SD-induced ABA signalling leads to a blockage of symplasmic intercellular communication (by closing plasmodesmata), which prevents growth-promoting signals[9] from entering the shoot apex[10–12].

Bud dormancy is also controlled by the widely-conserved TCP transcription factor BRANCHED1 (BRC1)[6,13]. Arabidopsis *BRC1,* expressed in axillary buds, activates ABA signalling, and downregulates genes associated with bud activation, including cell division and protein synthesis genes[14–16]. In poplar, SD-induced *BRC1*-like factors inhibit shoot apical bud growth by binding FT2 and antagonizing its growth-promoting activity[17]. In potato, *BRC1a,* one of the two BRC1 paralogs, also promotes bud dormancy both in aerial and stolon axillary buds [18,19]. The role of the second BRC1 paralog, *BRC1b,* remained to be studied.

We have now found that *BRC1b* acts as a multimodal tuberisation repressor in aerial axillary buds: it promotes bud dormancy, ABA signalling, and changes in plasmodesmata gene expression, which in turn limit sucrose unloading and SP6A access to axillary buds. BRC1b also interacts with, and antagonises the tuber-promoting SP6A protein thus reducing its activity in aerial nodes. These combined activities likely also promote the movement of SP6A to below-ground stolons. Furthermore, *BRC1b* prevents aerial buds from becoming strong sugar sinks in conflict with stolons, and promote sucrose allocation to stolon tips. All these actions help restrict tuberisation to stolons in the SD of winter as a critical plant survival strategy.

Results

Potato *BRC1b* is expressed in axillary buds and developing stolons. To elucidate the role of potato *BRC1b* we first studied its expression patterns. Quantitative real-time PCR (qPCR) of *BRC1b* mRNA levels in different tissues revealed that, like *BRC1a, BRC1b* mRNA accumulated in aerial and stolon axillary buds (**Fig. 1a**). However, unlike *BRC1a,* it also accumulated, at high levels, in developing stolons. Potato ssp. *andigena* and cv. Desiree transgenic lines carrying the *BRC1b* promoter fused to the *β-GLUCURONIDASE* (*GUS*) reporter coding sequence (*BRC1bpro:GUS*), and RNA *in situ* hybridisations using an antisense *BRC1b* mRNA specific probe performed in ssp. *andigena,* confirmed that *BRC1b* was active in aerial, stolon and tuber axillary buds (**Fig. 1b-i,k,l, Supplementary Fig. 1a-e**). *GUS* activity and *BRC1b* mRNA were also detectable at the shoot apex and vasculature of growing stolons and tubers (**Fig. 1d-j, Supplementary Fig. 1d,e,k**). In shoot apical, axillary and floral meristems, *BRC1b* expression was restricted to inner tissues (**Fig. 1i-l, Supplementary Fig. 1n**). In leaves of ssp. *andigena*, staining was initially generalised, but became progressively restricted to leaf margins and vasculature (**Supplementary Fig. 1f-h,j**), whereas in the cv. Desiree it was active mainly in the vasculature (**Supplementary Fig. 1i**).

These results support a potential role of *BRC1b* in the development of aerial and underground axillary buds and also during stolon, flower and leaf development.

Potato *BRC1b* prevents aerial bud tuberisation. To further analyse the function of *BRC1b*, we generated RNAi transgenic lines (RNAi) in which *BRC1b* mRNA levels were strongly reduced relative to the wild type (WT) (**Supplementary Fig. 2a,b**). We compared the phenotypes of RNAi lines with WT and plants bearing the empty vector, in LD (non-inducing, 16 h day/8 h night) and SD (tuber-inducing, 8 h day/16 h night) conditions, by using the SD-dependent ssp. *andigena* genotype.

RNAi lines had various leaf and branching phenotypes, above and below ground. For leaves, this involved simpler, more convex leaves than the controls (**Supplementary Fig. 3**). For branching, some lines developed a few more aerial branches than controls in LD (**Supplementary Fig. 4a**) and all had fewer, shorter and less branched stolons (**Supplementary Fig. 4b,c,d)**. After 6 weeks of transfer to SD, RNAi lines developed more aerial branches (**Supplementary Fig. 4e)** whereas their stolon number remained lower than in controls (**Supplementary Fig. 4f,g**).

The most dramatic phenotypes were seen in tuber formation. Under non-inductive LD, RNAi plants developed some underground tubers, a phenotype rarely observed in controls (**Fig. 2a, Supplementary Table 1**). Line #10 also displayed aerial tubers in LD (**Fig. 2d, Supplementary Fig. 5a,b, Supplementary Table 1**). Aerial nodes of some RNAi plants were also enlarged as compared with controls and seemed to accumulate starch (**Fig. 2e, Supplementary Fig. 5e,f**). Under inductive SD conditions, all control plants developed underground tubers at the tip of stolons as normal (**Fig. 2b, Supplementary Table 1**). In contrast, RNAi lines produced fewer underground tubers (**Fig. 2b**) with lower yield than controls **(Supplementary Fig. 6**), and some individuals failed to tuberise (**Supplementary Table 1**). Remarkably, all RNAi lines developed aerial tubers at axillary buds after four weeks in SD, a phenotype not observed in controls (**Fig. 2c,f,g, Supplementary Fig. 5 c,d**). Tubers were found in the lowermost and, more frequently, in the uppermost aerial nodes whereas the middle nodes developed fewer tubers (**Supplementary Fig. 7**). Furthermore, some aerial and underground RNAi tubers developed secondary tubers from tuber eyes (**Fig. 2g**). To further confirm these phenotypes we generated *BRC1b* RNAi lines in the cv. Desiree, and found that in this daylength-independent genotype RNAi lines also produced aerial tubers both in LD and SD as well as enlarged aerial nodes (**Supplementary Fig. 8**).

These results indicate that potato *BRC1b* has multiple effects on leaf and shoot branching and, in addition, it prevents aerial and underground tuber formation in LD and aerial tuberisation in SD.

***BRC1b* is required for axillary bud growth-to-dormancy transition in SD.** To elucidate the transcriptional changes underlying the aerial tuberisationphenotype of *BRC1b* RNAi plants, we compared their axillary bud transcriptomes with those of WT, using RNA sequencing. We took upper-bud samples (see Methods) of plants grown in LD, and after 2 days (2SD), 1 week (1wSD) and 2 weeks (2wSD) of transfer to SD (**Fig. 3a**). In WT, the highest number of differentially expressed genes (DEGs) was observed between LD and 2SD, confirming that the transition to SD is a major event in bud physiology (**Supplementary Fig. 9a,b**). In contrast, RNAi lines displayed a much-reduced response to the 2SD shift, suggesting that *BRC1b* plays an important role in SD (**Supplementary Fig. 9a,b**). Indeed, the number of DEGs between WT and RNAi samples increased from 2SD onwards (**Supplementary Fig. 9c**).

To identify the biological processes driving aerial tuber formation in the RNAi buds, we carried out a Gene Set Enrichment Analysis (GSEA[20]). First, we found that the potato orthologs of *BRC1*-dependent gene sets (identified in *Arabidopsis*[15]) were differentially expressed in the WT, but this response was reduced in RNAi buds (**Fig. 3b,** *BRC1*-dependent Up and Down, columns 2-4). This indicates that the genetic response to *BRC1* is conserved in potato.

In perennials SD promote bud dormancy[21,22], which involves repression of cell proliferation and induction of a carbon starvation syndrome, characterised by the activation of sugar-repressed genes[5,6,23]. To test these responses we used gene sets of dormant and active buds from *Arabidopsis*[5,24] and potato (dormant and sprouting potato tuber eyes[25]), sugar-repressed gene sets[26,27], and gene sets related to cell division and

protein synthesis. WT buds displayed a response typical of buds entering dormancy from 2SD, whereas this response was significantly reduced in RNAi lines even in LD (**Fig. 3b,** columns 1-4). Similarly, gene sets related to bud-activation, cell division and protein synthesis were significantly down-regulated in WT from 2SD onwards, but they were relatively much less repressed in RNAi buds (**Fig. 3b,** columns 1-4). This behaviour is illustrated by the expression patterns of the universal dormancy marker *DRM1*[28], and the *SHORT VEGETATIVE PHASE* (*SVP*) and *AIL1*-like genes, induced and repressed respectively during bud dormancy in perennials[29–32] (**Supplementary Fig. 10**).

In perennials, SD-induced transition to bud dormancy is associated to the blockage of symplasmic (plasmodesmata-mediated) intercellular trafficking, which prevents the access of growth-promoting molecules into the bud[10–12]. We tested a set of plasmodesmata-related genes[33] and found that, in RNAi buds, they were significantly less repressed than in WT (**Fig. 3b,** columns 1-4). Indeed, at 2wSD this gene set was induced in RNAi (**Fig. 3b,** column 10).

Altogether these results indicate that SD promote growth arrest and dormancy, a carbon starvation syndrome, and downregulation of plasmodesmata-related expression in aerial axillary buds, and that these responses require of the *BRC1b* function.

***BRC1b* is necessary for ABA, brassinosteroid and auxin responses in buds.** Next we investigated which hormonal pathways were affected by the SD treatment and/or the lack of *BRC1b*, by performing a GSEA of hormone-related datasets[5,34]. In WT, marker genes for ABA were induced in SD (**Fig. 3b**, columns 5-7) consistently with observations in other species that ABA signalling is induced in SD and is associated with bud dormancy[17,32,35–37]. By contrast, *BRC1b* RNAi buds displayed a reduced ABA response relative to the WT in SD (**Fig. 3b**, columns 2-4), in agreement with the proposed role of *BRC1*-like genes in promoting ABA signalling[16,24,38,39]. The ABA-related genes affected in RNAi buds included

genes involved in ABA biosynthesis, perception, signalling and response (**Supplementary Fig. 10).** At 2wSD, the ABA response in RNAi was not only reduced relatively to WT, but also repressed in absolute values, coinciding with the upregulation of the plasmodesmata-related gene set (**Fig. 3b**, column 10). This is consistent with the negative correlation between ABA signalling and plasmodesmata trafficking observed in poplar[12]. Likewise, brassinosteroid and IAA responses were induced in SD in the WT, but were mostly repressed in RNAi buds (**Fig. 3b,** columns 5-10).

The tuberisation pathway is activated in *BRC1b* RNAi buds. To better understand the timeline of responses leading to the RNAi aerial tuber phenotype we analysed early molecular markers for tuberisation. *GIBBERELLIN 2-OXIDASE1* (*Ga2OX1*), involved in the catabolism of gibberellins, an early marker of tuber induction and usually upregulated before swelling[3,40], was induced from 2SD in RNAi buds (**Supplementary Fig. 11,** columns 8-10). This suggests an early activation of the tuberisation pathway in RNAi buds. In general, active gibberellic acid (GA) inhibits tuber formation[40,41] and we found that GA gene markers were more repressed in RNAi than in WT in SD (**Fig. 3b,** columns 5-10**)**. Likewise, cytokinins (CK) promote tuberisation[41–44] and the gene set for CK markers was more induced in RNAi than in WT buds (**Fig. 3b,** columns 5-10**)**.

Another early tuberisation marker is the *SP6A* mRNA itself, which accumulates in tuberizing stolons due to a positive feed-back by the phloem-transported SP6A protein[3] and to sucrose-induced *SP6A* expression[45]. RNAi buds showed a significant induction of *SP6A* from 1wSD onwards (**Fig. 4a,** columns 9,10), and qPCR studies confirmed that expression of *SP6A* was further increased at 3wSD (**Fig. 4b**). In contrast, the expression of *SP5G*, which negatively regulates *SP6A* transcription[1,2], was reduced relative to WT in RNAi buds in SD (**Fig. 4c**). Another important tuberisation marker is the *SWEET11* gene that encodes a sucrose channel, and whose expression increases during tuberisation in

response to SP6A[45]. Consistently, *SWEET11* was upregulated in RNAi buds at 1wSD coinciding with *SP6A* upregulation (**Supplementary Fig. 12,** column 9). Finally, the tuberisation marker *BEL5*[46] was not found differentially expressed in RNAi buds (**Supplementary Fig. 12**), which is agreement with evidence that *BEL5* is an upstream transcriptional regulator of BRC1/TB1-like genes[47,48]. In summary, these results indicate that, in buds lacking *BRC1b,* the tuberisation pathway is induced already by 2SD, which results in visible aerial tubers after four weeks.

***BRC1b* RNAi buds accumulate high sucrose levels in SD.** Leaves are the major source of sucrose, the primary product of photosynthesis, and sugar transported to sink organs[49]. In active axillary buds, sucrose is cleaved by invertases into fructose and glucose, which is used for cell growth and proliferation[50]. In developing tubers, sucrose is instead hydrolysed by sucrose synthases (SuSy) into fructose and uridine diphosphate glucose (UDP-glucose), which is used for starch biosynthesis[49]. To investigate the sink/source status of WT and RNAi leaves and aerial buds, we quantified their carbohydrate (sucrose, glucose and starch) content in LD and 1wSD (**Fig. 5**).

In leaves, sucrose levels were similar in WT and RNAi lines-indicating that *BRC1b* does not impact the production of assimilates. Sucrose levels were much higher in LD - for both WT and RNAi lines- than in SD, probably due to a higher photosynthetic activity and/or lower sucrose export in LD (**Fig. 5a**)

. In contrast, in axillary buds, sucrose content was higher in SD than in LD in both genotypes (**Fig. 5d,g**), reflecting an enhanced sucrose transport from leaves to buds in SD. However, sucrose levels were significantly higher in RNAi than in WT buds, which suggest that RNAi buds are stronger sinks with increased ability to import and unload sucrose, in line with the induced expression of plasmodesmata-related genes in RNAi buds (**Fig. 3b**). Such an accumulation of sucrose did not result, however, in increased

starch levels in the axillary buds of either genotype, at least at 1wSD (**Fig. 5f,i**). It did however result in a markedly higher glucose content in the upper buds of RNAi in SD (**Fig. 5e**), which could reflect an increased invertase activity. Analyses of the invertase profiles in the time course samples (upper buds), confirmed differential induction of a vacuolar invertase and other invertases in RNAi in SD (**Supplementary Fig. 13,** columns 2-4).

Altogether these data suggest that in SD, *BRC1b* prevents the unloading of sucrose to axillary buds, thus making them weaker sinks than stolons where sucrose may be preferentially taken up.

BRC1b interacts with the tuberigen protein SP6A. In *Arabidopsis*, the FT protein, produced in leaves in LD, acts as a systemic signal to promote flowering in the shoot apical meristem. In the axillary buds, flowering is delayed due to a direct antagonistic interaction between BRC1 and the FT protein[51]. Likewise, in hybrid aspen the interaction between BRC1-2 and the FT-like factor FT2 prevents this from promoting apical growth in SD[17]. We hypothesised that in potato aerial axillary buds, the BRC1b protein could similarly bind and antagonise SP6A, an FT protein causing tuberisation, or alternatively bind SP5G and thus repress *SP6A* expression.

To test the interactions of these proteins we conducted yeast two-hybrid (Y2H) assays between the BRC1b, SP6A and SP5G proteins. We found that BRC1b interacted with both SP6A and SP5G, and that the TCP domain was necessary for this interaction (**Fig. 6a**). The BRC1b paralog, BRC1a^{L} [18,19], was also observed to interact with both proteins (**Supplementary Fig. 14**), but the binding affinity of BRC1a^{L}-SP6A was lower than that of BRC1b-SP6A.

Next we performed co-immunoprecipitation assays to confirm these interactions *in planta*. Constructs driving the expression of *BRC1b:HA* or *BRC1a^{L}:HA* were co-

infiltrated in *Nicotiana* leaves with constructs expressing either *SP6A:GFP* or *SP5G:GFP*, and the presence of these proteins was analysed after pull-down of protein extracts with anti-HA magnetic beads. These assays confirmed a strong interaction of BRC1b and SP6A (**Fig. 6b**), whereas interactions were much weaker for BRC1b-SP5G or $BRC1a^{L}$-SP6A, and no interaction was observed for $BRC1a^{L}$ and SP5G.

These findings demonstrate that BRC1b specifically interacts with SP6A and likely antagonises (via protein-protein interactions) its tuber-inducing activity in axillary buds, where BRC1b accumulates in WT.

Discussion

In potato, all axillary meristems (aerial and underground) can remain dormant or have the potential to develop into a branch, a stolon, or a tuber. The acquisition of these fates requires the activation of specific genetic programs, in response to positional and environmental cues. The ssp. *andigena* tubers are only formed in response to the SD of winter, and exclusively at stolon tips, below ground. This spatial restriction probably evolved to protect tubers from cold and animal foraging over the winter, and to ensure vegetative propagation the following spring.

In this study, we have shown that *BRC1b* is essential for efficient underground tuberisation: it prevents aerial buds from becoming sinks for assimilates in conflict with stolons, and thus facilitates stolon sink dominance. Accordingly, *BRC1b* silencing leads to formation of ectopic aerial tubers and reduced below-ground tuberisation. At the physiological and molecular level, the *BRC1b* loss-of-function syndrome comprises a collection of interconnected defects at aerial buds, which are detectable mainly in SD: impaired dormancy, increased CK signalling, limited ABA and GA signalling, increased expression of plasmodesmata-related genes, enhanced sucrose accumulation and higher *SP6A* levels.

One of the earliest features of RNAi aerial buds is their failure to enter dormancy, detectable as early as 2SD, which is consistent with the active-bud phenotype of *brc1* mutants of other species[52]. However, although active axillary buds are necessary[43], they are not sufficient to cause aerial-tuber phenotypes: *BRC1a* loss of function also causes bud activation, but plants lacking *BRC1a* do not display aerial tubers[18], which indicates that *BRC1b* plays a divergent, more specific role related to the tuberisation control. One key differential feature of BRC1b (as compared to BRC1a) is its unique capability to bind the SP6A protein, which probably inactivates this protein as it has been demonstrated in other developmental systems and species (see below).

BRC1b RNAi buds have higher CK and lower GA signalling, conditions that facilitate tuberisation *in vitro*[41,43,44,53,54]. The RNAi buds also have a reduced ABA response to SD. This is in agreement with the reported direct control of ABA signalling in buds by *BRC1/TB1 genes* [16,39]. Limited ABA signalling may in part explain the reduced bud dormancy of RNAi buds, as ABA is necesary to maintain bud growth arrest [7,8,12,15,24,36,55–57].

In hybrid aspen, SD-induced ABA signalling leads to changes in the plasmodesmata-related transcriptome, which in turn result in a blockage of the symplasmic intercellular communication. This prevents growth-promoting signals -such as FT-like proteins- from entering the apical bud[12,17]. In WT potato buds, SD-induced ABA signalling may likewise limit symplasmic transport of FT-like SP6A into aerial buds. In RNAi, low ABA signalling and high plasmodesmata gene expression (**Fig. 3**) can result in enhanced plasmodesmata trafficking of SP6A into axillary buds (**Fig. 7**). Likewise, the abnormally high levels of sucrose observed in RNAi buds can be explained by an increased sucrose uptake and unloading by symplasmic transport. This situation mirrors that of WT stolon tips, which during tuberisation undergo a switch from apoplastic to symplasmic sucrose unloading that enhances their sink potential. This is a key step in the regulation of resource allocation during tuber formation[58] that could take place

296 ectopically in aerial buds of RNAi plants, leading to major alterations in photoassimilate
297 distribution. Indeed, changes in the strength of individual sinks can greatly impact the
298 priority of assimilate partitioning[59], which in this case results in poor allocation of
299 assimilates to stolons. Remarkably, aerial tubers are more frequently formed in the
300 topmost nodes (where flowers are usually formed) indicating that sucrose fails to be
301 transported basipetally as it occurs during tuberisation (**Fig. 7, Supplementary Fig. 7**).
302 In WT, sucrose promotes the expression of *SP6A* in phloem and developing
303 tubers[45,54]. In RNAi buds, the increase of sucrose at 1wSD coincides with a strong
304 accumulation of *SP6A* mRNA, which can in part be sucrose-induced. The feed-back
305 regulation of *SP6A* by its own protein may account for additional increase in *SP6A*
306 mRNA levels[3]. SP6A can, in turn, boost sucrose unloading into the buds by a mechanism
307 similar to the one taking place in stolons: SP6A directly interacts with and antagonises the
308 sucrose transporter SWEET11 in the plasma membrane, thus preventing sucrose
309 apoplastic leakage, and facilitating symplastic transport[45]. This cross-talk between sucrose
310 and *SP6A* can trigger the tuberisation pathway in *BRC1b* RNAi aerial buds (**Fig. 7a**). In
311 WT, high levels of BRC1b that directly interacts with SP6A creates a buffering mechanism
312 that prevents the initiation of this positive feedback. Furthermore, BRC1b activates
313 *SWEET11* (**Supplementary Fig. 13**, columns 1,2), which facilitates apoplastic transport[45].
314 A remarkable degree of genetic conservation is found between the pathways that
315 control flowering time in annuals, apical growth (vs. dormancy) in perennials, and tuber
316 formation in potato[1–3,17,60,61] (this work). Notably, all are sugar-demanding processes that
317 take place in strong sink organs. In those sinks, sucrose supports growth and activates FT-
318 like genes, which ultimately regulate these developmental pathways[45]. In contrast, BRC1-
319 like genes, repressed by sugar[5,6] and active under energy-limiting conditions, promote
320 energy-saving mechanisms, and further antagonise these developmental pathways in part
321 by negatively modulating the activity of FT-like genes via direct protein-protein

322 interactions, but probably also through other mechanisms[17,51] (this work). This reveals the
323 existence of a widely conserved FT-BRC1 genetic module, perhaps evolved in early
324 angiosperms, in which FT promotes processes requiring sucrose and energy, whereas
325 BRC1 genes activate energy-saving programs[5,6]. The positive (*FT*) and negative (*BRC1*)
326 regulation of these genes by sucrose or sucrose derivatives, and the direct interaction and
327 mutual regulation of their proteins would directly integrate the metabolic status of the
328 plant with developmental decisions that require a tightly regulated use and allocation of
329 photoassimilates.
330
331 **Methods**
332 **Plant material and growth conditions**
333 All experiments were carried out using plants from *S. tuberosum* ssp. *andigena*
334 7540 and, when indicated, also *S. tuberosum* L. cv. Désirée.
335 Plants were propagated *in vitro* from single-node stem cuttings on Murashige and Skoog
336 (MS) medium containing 2% sucrose and 0.8% agar, in chambers at 21ºC in LD
337 photoperiod (16h light -8h dark, PAR 90 µmol m^2s^{-1}). Once they had developed five
338 visible nodes they were cut at the base and transferred to new jars for 5-7 days for
339 rooting. Synchronised rooted cuttings were then transferred to soil (ratio
340 substrate:vermiculite, 3:1) with 5 basal nodes buried. Plants were covered with pierced
341 transparent plastic cups for 24 hours and then uncovered. Plants were grown in the
342 greenhouse at 21-24ºC, in LD, natural light supplemented with Na lamps when required
343 (intensity <110 µmol·m2·s-1). They were watered with a nutritive solution (6.25 mM
344 KNO_3, 12.5 mM $Ca(NO_3)_24H_2O$, 1 mM KH_2PO_4, 1 mM $MgSO_4$, 0.016 g/L micronutrients
345 Kelamix™ and 0.08 g/l Hortrilon™) once a week.
346 Plants used for phenotypic or expression analysis (qPCR or RNA-seq) in LD vs SD were
347 first grown in the greenhouse and then transferred to a growth chamber with similar

temperature and light conditions and adequate photoperiod. For the co-immunoprecipitation assays, *Nicotiana benthamiana* plants were grown in the greenhouse in similar conditions**.**

Plant phenotyping

Phenotypic analyses in LD and SD were done as follows: 10 synchronised plants of each genotype, with 6 visible nodes, were transferred to soil; 5 nodes were buried to produce stolons. For LD phenotyping, plants were grown for 16 weeks in the greenhouse; for SD phenotyping, plants were grown for 10 weeks in the greenhouse (LD) and then transferred to a growth chamber in SD (8h light, 16h dark) for 6 weeks. Branches and stolons were considered when longer than 1cm. All tubers were considered. For Désirée cv. phenotypic analysis, 20 *BRC1b* RNAi lines were studied. Phenotypes were analysed when WT plants became senescent. At this time transgenic plants were still green.

For the leaf phenotype, plants were grown for 6 weeks in the greenhouse and then leaves from even nodes were collected starting from the lowest nodes.

Constructs

Full-length *BRC1b* (PGSC0003DMG400004054) and *BRC1a* (PGSC0003DMG400005705) coding sequences (Désirée cv. background) cloned in pDONR207 and *SP6A* and *SP5G* (ssp. *andigena* background) coding sequences cloned in pENTR/D-TOPO were available[2,18]. Vectors for all assays were generated by LR recombination using Gateway LR clonase II (Invitrogen) according to manufacturer's instructions.

For the *proBRC1b:GUS* construct, a genomic fragment comprising 2.5 kb upstream the ATG was amplified from genomic DNA of Désirée cv. plants with taq Phusion polymerase (New England BioLabs, primers in **Supplementary Table 2**). The PCR

fragment was cloned in pGEM-t Easy (Promega), re-amplified by PCR with primers with attB tails and BP-cloned into pDONR207 (Invitrogen). The fragment was then LR-cloned into the destination vector pGWB3[62].

To generate the *BRC1b* RNAi constructs, *BRC1b*-specific PCR products (168 bp) obtained with primers indicated (**Supplementary Table 2**) were cloned into the vector pHANNIBAL (CSIRO) using restriction sites BamHI/ClaI and XhoI/KpnI for the first and second cloning, respectively as described in Martín-Trillo et al. (2011)[19]. The pHANNIBAL cassettes were digested with NotI and subcloned in the NotI site of the binary vector pART27[63]. For the transgenic control lines an empty pHANNIBAL cassette subcloned in pART27 was used.

For the Y2H assays, coding sequences were integrated into pGADT7-GW or pGBKT7-GW (YTH assays; Invitrogen) by LR cloning. The truncated forms of *BRC1a*^{L} and *BRC1b* were cloned in pDONR207 after amplification using primers indicated in **Supplementary Table 2**. For the co-immunoprecipitation, expression vectors containing. *UBQ10pro:BRC1a:6XHA*, *UBQ10pro:BRC1b:6XHA*, *UBQ10pro:SP5G:Citrin* and *UBQ10pro:SP6A:Citrin* were generated by triple Gateway cloning using the destination vector pB7mG34GW (TAIR accession number: Vector:6530643175)[64]. The control construct *UBQ10pro:Citrin:c-Myc(NLS):Citrin* was available[18].

Generation of transgenic plants

Binary vectors were transformed into the *Agrobacterium tumefaciens* strain AGL-0. To generate stable transgenic potato plants, leaves were transformed according to Amador et al. (2001)[65]. *BRC1b* silencing and *PDK* intron expression (intron of the hairpin) were confirmed by qPCR in axillary buds using primers indicated in **Supplementary Table 2**. *BRC1b* RNAi lines #5, #10 and #19 were selected in ssp. *andigena* background and lines #13, #27, #36 and #40 in Désirée cv.

400 **_GUS_ staining**

401 *GUS* staining was conducted as described[66].

402

403 **RNA *in situ* hybridisation**

404 RNA *in situ* hybridisation and images acquisition were performed as described by Seibert
405 et al. 2020[67]. Tissues were collected at the end of the day. Samples were fixed with
406 Formaldehyde-Acetic acid–Ethanol, dehydrated with ethanol and infiltrated with paraffin
407 (Paraplast, Leica). After infiltration, samples were processed in an embedding station
408 (EG1160, Leica). 8-µm sections were obtained with a rotary microtome (RM2265, Leica),
409 and transferred to polysine-coated slides (Roth, Karlsruhe, Germany).
410 A *BRC1b* full-length probe was generated from its cDNA and cloned into the pGEM®-T
411 Easy Vector (Promega), and synthesised with a DIG RNA Labeling Kit (Roche).

412

413 **Stem section**

414 Stems from the basal part (between second and fourth node) of one-month-old WT and
415 *BRC1b* RNAi line #5 plants were cut and placed in cold 90% Acetone and fixed in 4%
416 glutaraldehyde. Deshydration, staining, resin inclusion and sectioning were done as
417 described Chevalier et al. (2014)[68].

418

419 **Y2H assays**

420 Vectors were transformed in yeast strain AH109. Yeast interaction assays were carried out
421 in selective medium deficient in leucine, tryptophan, adenine and histidine (SD-LWAH)
422 with 20 mM or 50 mM 3-amino-1,2,4-triazole (3-AT) as described Nieto et al. (2015)
423 Yeast colony growth was compared to their equivalent in SD-LW plates (positive growth
424 controls). Each combination was analysed three times.

425

CoIP assays

Constructs were transformed in the *Agrobacterium tumefaciens* strain AGL-0. Overnight cultures of *Agrobacterium* were resuspended in 10 mM MES (pH 5.5), 10 mM MgCl2, and 150 mM acetosyringone at an OD_{600nm} = 0.5 and incubated 3 hours at room temperature. Identical volumes of each resuspended culture were mixed for co-infiltrations in *N. benthamiana* leaves. Samples were collected 24 hours after infiltration. Co-immunoprecipitation was performed as described Nieto et al. (2015)[69].

Starch and sugar measurements

For starch and sugar measurements plants were grown in the greenhouse for 6 weeks and transferred to a LD growth chamber for one week to set up dawn time. Leaves and axillary buds were sampled one hour after dawn (ZT1) and flash frozen in N2(l). After collecting the LD samples, the chamber photoperiod was set to SD conditions and samples were collected 1 week later. Material termed "Upper axillary buds" were the four aerial axillary buds bellow the third visible node counting from the apex. Material termed "Lower axillary buds" were from the first four nodes starting from ground level. Leaves were from these same lower nodes. Biological replicates are pooled material from 4 plants. Leaves were ground in the mortar and axillary buds in Qiagen TissueLyser. An aliquot of the powder was transferred to a 2ml-cap tube and weighted in a precision scale for normalisation of sugar/starch content. Sugar and starch extraction is based on Smith and Zeeman (2006)[70]. 1ml of ethanol 80% was added to the ground tissue and the tubes were place in a thermo-shaker at 80°C for 1 hour. After centrifugation pellet was washed twice. The pellet containing insoluble starch was dried and resuspended in 1ml of Milli-Q water. Starch was solubilised by heating the tube at 100°C in a thermo-shaker for 1 hour. Supernatants of the first wash containing the reducing sugars were dried in a

Speedvac and the pellet was resuspended in 200µl of milli-Q water. Starch, sucrose and glucose were quantified with the starch Saccharose/D-Glucose kit (Roche/r-Biopharm).

Experimental design of RNA-seq time course and qPCR experiments

Plants were grown in the greenhouse for 6 weeks, and then placed in a LD growth chamber for 1 week, after which samples for the LD time point were collected. Growth chamber photoperiod was then set to SD by bringing the night-time forward. The following day corresponds to the first day in SD. Samples were collected at 2 days (SD2), 1 week (1W), 2 weeks (2W) and 3 weeks (3W) (only for qPCR). All samples were obtained at one hour after dawn (ZT1). Upper axillary buds (see Starch and sugar measurements) (those most likely to produce tubers) were collected.

RNA extraction and RNA-seq analysis

Bud-containing stem nodes were flash-frozen in N2(l), subsequently dissected at 4ºC, and then ground in the Qiagen TissueLyser. Three biological replicates (each a bud pool from four plants) were collected. RNA was extracted with FavorPrep™ Plant Total RNA Mini Kit (FAVORGEN). DNA was digested in the column with RNase-free DNase I (Roche). Samples were sent for sequencing at BGI Genomics (Beijing, China).

24 samples of *Solanum tuberosum* ssp. *andigena* were sequenced on a BGISEQ-500 Platform, generating about 7.01 Gb per sample. The average genome-mapping rate was 83.28% and the average gene-mapping rate was 69.20%. RNA-Seq paired-ends reads were filtered using SOAPnuke v1.5.2[71] to remove reads with adaptors, having more than 5% unknown bases or with poor base quality (more than 20% bases having quality <15). The cleaned reads were then aligned to the PGSC_DM_v4.03_pseudomolecules reference genome[72], available at http://solanaceae.plantbiology.msu.edu/pgsc_download.shtml) using HISAT v2.0.4[73] with

477 the *sensitive* mode, options no-discordant and no-mixed, minimum fragment size 1 and
478 maximum fragment size to 1000.
479 Reads per gene quantification for each sample was performed using the FeatureCounts
480 function implemented in the R package Rsubread v2.0.0[74] with the
481 PGSC_DM_V403_genes file.gff from
482 http://solanaceae.plantbiology.msu.edu/pgsc_download.shtml as genome annotation and
483 parameter is PairedEnd=TRUE. Then, Differentially Expressed Genes were calculated for
484 each comparison between conditions using the R package DESeq2 v1.26.0[75] with default
485 values. RNA-seq data are available at the NCBI GEO database with Accession Code
486 GSE155774.
487
488 **Real-time qPCR**
489 *SP5G* is not included in the current version of the genome annotation
490 (PGSC_DM_V403_genes[72]) and its expression was therefore analysed by qPCR. 1µg total
491 RNA of axillary buds was used for reverse transcription using the High-Capacity cDNA
492 Reverse Transcription Kit from AppliedBiosystem following manufacturer's instruction.
493 cDNA was diluted 7 times before performing qPCR. GoTaq qPCR Master Mix (Promega)
494 and the Applied Biosystems 7500 real-time PCR system were used to perform the qPCRs.
495 Primers used are in **Supplemental Table 2**. *StACTIN8* was used as reference gene. Three
496 technical replicates were performed for each of the three biological replicates. The gene
497 relative expressions were calculated using Q-base v1.3.5[76].
498
499 **Gene Set Enrichment Analysis**
500 The tests of overrepresentation of the different gene sets were carried out with the Gene
501 Set Enrichment Analysis (GSEA[20]) method (version 3.0) as described in Tarancon et al.
502 (2017)[5]. All the gene sets defined for this study were used in Tarancon et al. (2017)[5],

503 excepting the gene sets for Tuber eyes dormancy and sprouting[25] and *A. thaliana*
504 Plasmodesmata genes[33].
505 All gene sets are available in **Supplemental Table 3**: Potato putative orthologs of *A.*
506 *thaliana* genes were determined according to the potato genome annotation computed by
507 PHYTOZOME (Stuberosum_448_v4.03.annotation_info; based on genome version v4.03,
508 best hits in BLASTP alignment to A. thaliana TAIR10). When several potato gene loci
509 were associated to a single Arabidopsis gene, all of them were included in the gene set.
510 The GSEA method evaluates whether these genes occur preferentially toward the top or
511 bottom of a ranked list. Complete results are in
512 http://bioinfogp.cnb.csic.es/files/projects/nicolas_et_al_2020_gsea
513

514 **References**

515 1. Kloosterman, B. *et al.* Naturally occurring allele diversity allows potato cultivation
516 in northern latitudes. *Nature* **495**, 246–250 (2013).
517 2. Abelenda, J. A., Cruz-Oró, E., Franco-Zorrilla, J. M. & Prat, S. Potato
518 StCONSTANS-like1 Suppresses Storage Organ Formation by Directly Activating
519 the FT-like StSP5G Repressor. *Curr. Biol.* **26**, 872–881 (2016).
520 3. Navarro, C. *et al.* Control of flowering and storage organ formation in potato by
521 FLOWERING LOCUS T. *Nature* **478**, 119–22 (2011).
522 4. Teo, C.-J., Takahashi, K., Shimizu, K., Shimamoto, K. & Taoka, K. Potato Tuber
523 Induction is Regulated by Interactions Between Components of a Tuberigen
524 Complex. *Plant Cell Physiol.* **58**, 365–374 (2017).
525 5. Tarancón, C., González-Grandío, E., Oliveros, J. C., Nicolas, M. & Cubas, P. A
526 Conserved Carbon Starvation Response Underlies Bud Dormancy in Woody and
527 Herbaceous Species. *Front. Plant Sci.* **8**, 1–21 (2017).
528 6. Martín-Fontecha, E. S., Tarancón, C. & Cubas, P. To grow or not to grow, a power-

529 saving program induced in dormant buds. *Curr. Opin. Plant Biol.* **41**, 102–109
530 (2018).
531 7. Ruttink, T. *et al.* A Molecular Timetable for Apical Bud Formation and Dormancy
532 Induction in Poplar. *Plant Cell* **19**, 2370–2390 (2007).
533 8. Díaz-Riquelme, J., Grimplet, J., Martínez-Zapater, J. M. & Carmona, M. J.
534 Transcriptome variation along bud development in grapevine (Vitis vinifera L.).
535 *BMC Plant Biol.* **12**, 181 (2012).
536 9. Bohlenius, H. CO/FT Regulatory Module Controls Timing of Flowering and
537 Seasonal Growth Cessation in Trees. *Science.* **312**, 1040–1043 (2006).
538 10. Rinne, P. L. H. & Van der Schoot, C. Symplasmic fields in the tunica of the shoot
539 apical meristem coordinate morphogenetic events. *Development* **125**, 1477–1485
540 (1998).
541 11. Rinne, P. L. H., Kaikuranta, P. M. & Van Schoot, C. Der. The shoot apical
542 meristem restores its symplasmic organization during chilling-induced release from
543 dormancy. *Plant J.* **26**, 249–264 (2001).
544 12. Tylewicz, S. *et al.* Photoperiodic control of seasonal growth is mediated by ABA
545 acting on cell-cell communication. *Science.* **360**, 212–215 (2018).
546 13. Wang, M. *et al.* BRANCHED1: A Key Hub of Shoot Branching. *Front. Plant Sci.* **10**,
547 1–12 (2019).
548 14. Aguilar-Martínez, J. A., Poza-Carrión, C. & Cubas, P. Arabidopsis BRANCHED1
549 acts as an integrator of branching signals within axillary buds. *Plant Cell* **19**, 458–
550 72 (2007).
551 15. Gonzalez-Grandio, E., Poza-Carrion, C., Sorzano, C. O. S. & Cubas, P.
552 BRANCHED1 Promotes Axillary Bud Dormancy in Response to Shade in
553 Arabidopsis. *Plant Cell* **25**, 834–850 (2013).
554 16. González-Grandío, E. *et al.* Abscisic acid signaling is controlled by a

BRANCHED1/HD-ZIP I cascade in Arabidopsis axillary buds. *Proc. Natl. Acad. Sci.* **114**, E245–E254 (2017).

17. Maurya, J. P. *et al.* Branching Regulator BRC1 Mediates Photoperiodic Control of Seasonal Growth in Hybrid Aspen. *Curr. Biol.* **30**, 122-126.e2 (2020).

18. Nicolas, M., Rodríguez-Buey, M. L., Franco-Zorrilla, J. M. & Cubas, P. A Recently Evolved Alternative Splice Site in the BRANCHED1a Gene Controls Potato Plant Architecture. *Curr. Biol.* **25**, 1799–1809 (2015).

19. Martín-Trillo, M. *et al.* Role of tomato BRANCHED1-like genes in the control of shoot branching. *Plant J.* **67**, 701–714 (2011).

20. Subramanian, A. *et al.* Gene set enrichment analysis: A knowledge-based approach for interpreting genome-wide expression profiles. *Proc. Natl. Acad. Sci. U. S. A.* **102**, 15545–15550 (2005).

21. Paul, L. K., Rinne, P. L. H. & van der Schoot, C. Shoot meristems of deciduous woody perennials: self-organization and morphogenetic transitions. *Curr. Opin. Plant Biol.* **17**, 86–95 (2014).

22. Kramer, paul J. Effect of variation in length of say on growth and dormancy of trees. *Plant Physiol.* **11**, 127–137 (1936).

23. Thimm, O. *et al.* MAPMAN: A user-driven tool to display genomics data sets onto diagrams of metabolic pathways and other biological processes. *Plant J.* **37**, 914–939 (2004).

24. González-Grandío, E. & Cubas, P. Identification of gene functions associated to active and dormant buds in Arabidopsis. *Plant Signal. Behav.* **9**, e27994 (2014).

25. Campbell, M., Suttle, J., Douches, D. S. & Buell, C. R. Treatment of potato tubers with the synthetic cytokinin 1-(α-ethylbenzyl)-3-nitroguanidine results in rapid termination of endodormancy and induction of transcripts associated with cell proliferation and growth. *Funct. Integr. Genomics* **14**, 789–799 (2014).

581 26. Gonzali, S. *et al.* Identification of sugar-modulated genes and evidence for in vivo
582 sugar sensing in Arabidopsis. *J. Plant Res.* **119**, 115–123 (2006).
583 27. Osuna, D. *et al.* Temporal responses of transcripts, enzyme activities and
584 metabolites after adding sucrose to carbon-deprived Arabidopsis seedlings. *Plant J.*
585 **49**, 463–491 (2007).
586 28. Falavigna, V. da S., Guitton, B., Costes, E. & Andrés, F. I want to (Bud) break free:
587 The potential role of DAM and SVP-like genes in regulating dormancy cycle in
588 temperate fruit trees. *Front. Plant Sci.* **9**, 1–17 (2019).
589 29. Bielenberg, D. G. *et al.* Sequencing and annotation of the evergrowing locus in
590 peach [Prunus persica (L.) Batsch] reveals a cluster of six MADS-box transcription
591 factors as candidate genes for regulation of terminal bud formation. *Tree Genet.*
592 *Genomes* **4**, 495–507 (2008).
593 30. Sasaki, R. *et al.* Functional and expressional analyses of PmDAM genes associated
594 with endodormancy in Japanese apricot. *Plant Physiol.* **157**, 485–497 (2011).
595 31. Wu, R. *et al.* SVP-Like MADS box genes control dormancy and budbreak in apple.
596 *Front. Plant Sci.* **8**, 1–11 (2017).
597 32. Singh, R. K. *et al.* A genetic network mediating the control of bud break in hybrid
598 aspen. *Nat. Commun.* **9**, 4173 (2018).
599 33. Fernandez-Calvino, L. *et al.* Arabidopsis Plasmodesmal Proteome. *PLoS One* **6**,
600 e18880 (2011).
601 34. Nemhauser, J. L., Hong, F. & Chory, J. Different plant hormones regulate similar
602 processes through largely nonoverlapping transcriptional responses. *Cell* **126**,
603 467–75 (2006).
604 35. Rinne, P., Saarelainen, A. & Junttila, O. Growth cessation and bud dormancy in
605 relation to ABA level in seedlings and coppice shoots of Betula pubescens as
606 affected by a short photoperiod, water stress and chilling. *Physiol. Plant.* **90**, 451–

458 (1994).

36. Karlberg, A. *et al.* Analysis of global changes in gene expression during activity-dormancy cycle in hybrid aspen apex. *Plant Biotechnol.* **27**, 1–16 (2010).

37. Chmielewski, F., Gotz, K., Homann, T., Huschek, G. & Rawel, H. Identification of Endodormancy Release for Cherries (Prunus Avium L.) by Abscisic Acid and Sugars. *J. Hortic.* **04**, (2017).

38. Finkelstein, R. Abscisic Acid Synthesis and Response. *Arab. B.* **11**, e0166 (2013).

39. Dong, Z. *et al.* The regulatory landscape of a core maize domestication module controlling bud dormancy and growth repression. *Nat. Commun.* **10**, 3810 (2019).

40. Kloosterman, B. *et al.* StGA2ox1 is induced prior to stolon swelling and controls GA levels during potato tuber development. *Plant J.* **52**, 362–373 (2007).

41. Abelenda, J. A., Navarro, C. & Prat, S. Flowering and tuberization: A tale of two nightshades. *Trends Plant Sci.* **19**, 115–122 (2014).

42. Palmer, C. E. & Smith, O. E. Cytokinins and Tuber Initiation in the Potato Solanum tuberosum L. *Nature* **221**, 279–280 (1969).

43. Eviatar-Ribak, T. *et al.* A Cytokinin-Activating Enzyme Promotes Tuber Formation in Tomato. *Curr. Biol.* **23**, 1057–1064 (2013).

44. Guivarc'h, A. *et al.* Local expression of the ipt gene in transgenic tobacco (Nicotiana tabacum L. cv. SR1) axillary buds establishes a role for cytokinins in tuberisationand sink formation. *J. Exp. Bot.* **53**, 621–629 (2002).

45. Abelenda, J. A. *et al.* Source-Sink Regulation Is Mediated by Interaction of an FT Homolog with a SWEET Protein in Potato. *Curr. Biol.* 1–9 (2019). doi:10.1016/j.cub.2019.02.018

46. Chen, H. Interacting Transcription Factors from the Three-Amino Acid Loop Extension Superclass Regulate Tuber Formation. *Plant Physiol.* **132**, 1391–1404 (2003).

633 47. Sharma, P., Lin, T. & Hannapel, D. J. Targets of the StBEL5 Transcription Factor
634 Include the FT Ortholog StSP6A. *Plant Physiol.* **170**, 310–324 (2016).
635 48. Bolduc, N. *et al.* Unraveling the KNOTTED1 regulatory network in maize
636 meristems. *Genes Dev.* **26**, 1685–1690 (2012).
637 49. Fernie, A. R. *et al.* Synchronization of developmental, molecular and metabolic
638 aspects of source–sink interactions. *Nat. Plants* **6**, 55–66 (2020).
639 50. Ruan, Y.-L. Sucrose Metabolism: Gateway to Diverse Carbon Use and Sugar
640 Signaling. *Annu. Rev. Plant Biol.* **65**, 33–67 (2014).
641 51. Niwa, M. *et al.* BRANCHED1 Interacts with FLOWERING LOCUS T to Repress the
642 Floral Transition of the Axillary Meristems in Arabidopsis. *Plant Cell* **25**, 1228–
643 1242 (2013).
644 52. Nicolas, M. & Cubas, P. The Role of TCP Transcription Factors in Shaping Flower
645 Structure, Leaf Morphology, and Plant Architecture. in *Plant Transcription Factors*
646 (ed. Gonzalez, D. H.) 249–267 (Elsevier, 2016). doi:10.1016/B978-0-12-800854-
647 6.00016-6
648 53. Hoque, M. E. In vitro tuberisationin potato (Solanum tuberosum L .). *Plant Omi. J.*
649 **3**, 7–11 (2010).
650 54. Xu, X., van Lammeren AA, Vermeer, E. & Vreugdenhil, D. The role of gibberellin,
651 abscisic acid, and sucrose in the regulation of potato tuber formation in vitro. *Plant*
652 *Physiol.* **117**, 575–84 (1998).
653 55. Reddy, S. K., Holalu, S. V, Casal, J. J. & Finlayson, S. a. Abscisic acid regulates
654 axillary bud outgrowth responses to the ratio of red to far-red light. *Plant Physiol.*
655 **163**, 1047–1058 (2013).
656 56. Yao, C. & Finlayson, S. A. Abscisic Acid Is a General Negative Regulator of
657 Arabidopsis Axillary Bud Growth. *Plant Physiol.* **169**, 611–626 (2015).
658 57. Penfield, S. & King, J. Towards a systems biology approach to understanding seed

dormancy and germination. *Proc. R. Soc. B Biol. Sci.* **276**, 3561–3569 (2009).

58. Viola, R. *et al.* Tuberisationin Potato Involves a Switch from Apoplastic to Symplastic Phloem Unloading. *Plant Cell* **13**, 385 (2001).

59. Ho, L. C. Metabolism and Compartmentation of Imported Sugars in Sink Organs in Relation to Sink Strength. *Annu. Rev. Plant Physiol. Plant Mol. Biol.* **39**, 355–378 (1988).

60. Andrés, F. & Coupland, G. The genetic basis of flowering responses to seasonal cues. *Nat. Rev. Genet.* **13**, 627–639 (2012).

61. Maurya, J. P. & Bhalerao, R. P. Photoperiod- and temperature-mediated control of growth cessation and dormancy in trees: A molecular perspective. *Ann. Bot.* **120**, 351–360 (2017).

62. Nakagawa, T. *et al.* Development of series of gateway binary vectors, pGWBs, for realizing efficient construction of fusion genes for plant transformation. *J. Biosci. Bioeng.* **104**, 34–41 (2007).

63. Gleave, A. P. A versatile binary vector system with a T-DNA organisational structure conducive to efficient integration of cloned DNA into the plant genome. *Plant Mol. Biol.* **20**, 1203–1207 (1992).

64. Karimi, M., De Meyer, B. & Hilson, P. Modular cloning in plant cells. *Trends Plant Sci.* **10**, 103–5 (2005).

65. Amador, V., Monte, E., García-Martínez, J.-L. & Prat, S. Gibberellins Signal Nuclear Import of PHOR1, a Photoperiod-Responsive Protein with Homology to Drosophila armadillo. *Cell* **106**, 343–354 (2001).

66. Sessions, A., Weigel, D. & Yanofsky, M. F. The Arabidopsis thaliana MERISTEM LAYER 1 promoter specifies epidermal expression in meristems and young primordia. *Plant J.* **20**, 259–63 (1999).

67. Seibert, T., Abel, C. & Wahl, V. Flowering time and the identification of floral

marker genes in Solanum tuberosum ssp. andigena. *J. Exp. Bot.* **71**, 986–996 (2020).

68. Chevalier, F., Iglesias, S. M., Sánchez, Ó. J., Montoliu, L. & Cubas, P. Plastic Embedding of Stem Sections. *Bio-protocol* **4**, 1–7 (2014).

69. Nieto, C., López-Salmerón, V., Davière, J. & Prat, S. Report ELF3-PIF4 Interaction Regulates Plant Growth Independently of the Evening Complex. *Curr. Biol.* 187–193 (2015). doi:10.1016/j.cub.2014.10.070

70. Smith, A. M. & Zeeman, S. C. Quantification of starch in plant tissues. *Nat. Protoc.* **1**, 1342–1345 (2006).

71. Chen, Y. *et al.* SOAPnuke: a MapReduce acceleration-supported software for integrated quality control and preprocessing of high-throughput sequencing data. *Gigascience* **7**, 1–6 (2018).

72. Sharma, S. K. *et al.* Construction of reference chromosome-scale pseudomolecules for potato: Integrating the potato genome with genetic and physical maps. *G3 Genes, Genomes, Genet.* **3**, 2031–2047 (2013).

73. Kim, D., Langmead, B. & Salzberg, S. L. HISAT: A fast spliced aligner with low memory requirements. *Nat. Methods* **12**, 357–360 (2015).

74. Liao, Y., Smyth, G. K. & Shi, W. The R package Rsubread is easier, faster, cheaper and better for alignment and quantification of RNA sequencing reads. *Nucleic Acids Res.* **47**, (2019).

75. Love, M. I., Huber, W. & Anders, S. Moderated estimation of fold change and dispersion for RNA-seq data with DESeq2. *Genome Biol.* **15**, 1–21 (2014).

76. Hellemans, J., Mortier, G., De Paepe, A., Speleman, F. & Vandesompele, J. qBase relative quantification framework and software for management and automated analysis of real-time quantitative PCR data. *Genome Biol.* **8**, R19 (2007).

Acknowledgements

Research of Cubas´ group was funded by the Spanish Ministry of Economy (MINECO) and fondos FEDER [grants BIO2014-57011-R, BIO2017-84363-R]. Research of Prat´s group was funded by MINECO and fondos FEDER [grants BIO2015-73019-EXP, COSMIC EIG CONCERT-Japan]. Research in Wahl´s group was supported by the BMBF (031B0191), the DFG (SPP1530: WA3639/1-2, 2-1) and the Max-Planck-Society. MN was an Excelence Severo Ochoa (MINECO) postdoctoral researcher. We thank Tanja Seibert for help with *in situ* hybridisations and photography, and Desmond Bradley and José A Abelenda for constructive criticisms of the manuscript.

Figures

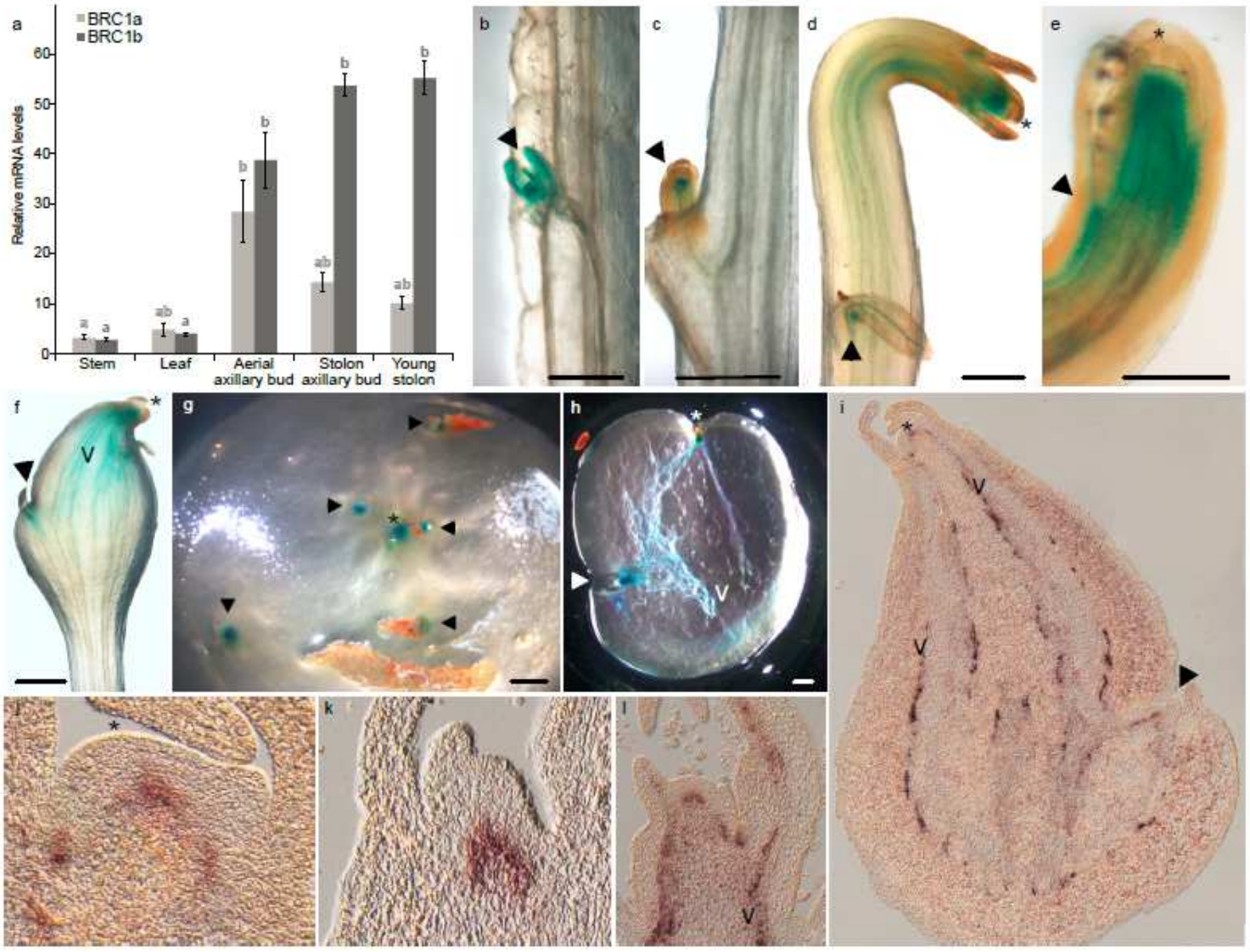

Figure 1

Expression of BRC1b during potato (ssp. andigena) development. a, BRC1a and BRC1b relative mRNA levels in different organs quantified by qPCR. Results are mean of three biological replicates. Error bars are SEM. Different letters above bars indicate significant differences among means (one-way ANOVA, $P < 0.05$). b-h, GUS histological activity of transgenic plants carrying a 2.5kb-BRC1bpro:GUS construct; i-l BRC1b RNA in situ hybridizations with a probe complementary to BRC1b mRNA. b, Aerial axillary bud. c, Stolon axillary bud. d, Stage-1 stolon. e, Close up of a stage-1 stolon apex. f, Stage-3 developing tuber. g, Close up of a tuber apical region. Apical (asterisk) and axillary buds (arrowheads) show GUS activity. h, Tuber section showing GUS signal in the apical and axillary buds and vasculature (v). i, Longitudinal section of a stage-4 developing tuber. j, Shoot apical meristem close-up of the developing-tuber shown in i. k, Axillary bud of a stage-1 stolon. l, Aerial axillary bud. Arrowheads indicate axillary buds, asterisks, shoot apices, v, vascular tissue. Scale bars = 1mm.

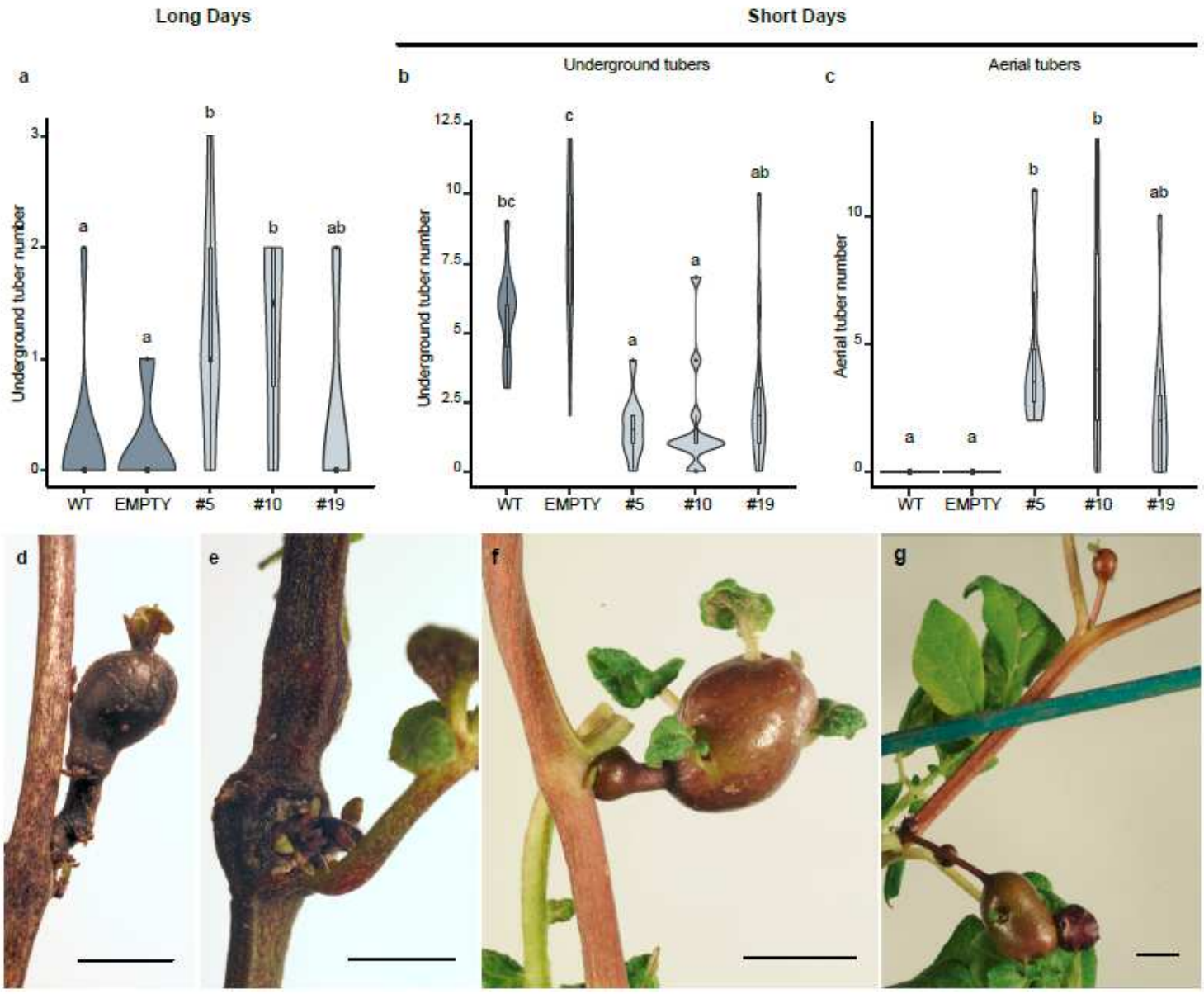

Figure 2

Aerial tuber phenotype of potato (ssp. andigena) BRC1b RNAi lines. Violin plots depicting the number of underground tubers (a,b) and aerial tubers (c) of plants grown in LD (a) or in LD followed by 6 weeks in SD (b,c). WT, wild type; EMPTY, control plants carrying an empty RNAi vector, and 3 BRC1b RNAi lines #5, #10 and #19. N=10; letters designate significant differences among means (one-way ANOVA, $P < 0.05$). Aerial tuber (d) and swollen node (e) of BRC1b RNAi plants grown in LD. f,g, aerial tubers of BRC1b RNAi plants grown in LD followed by 6 weeks in SD. Scale bars = 1cm.

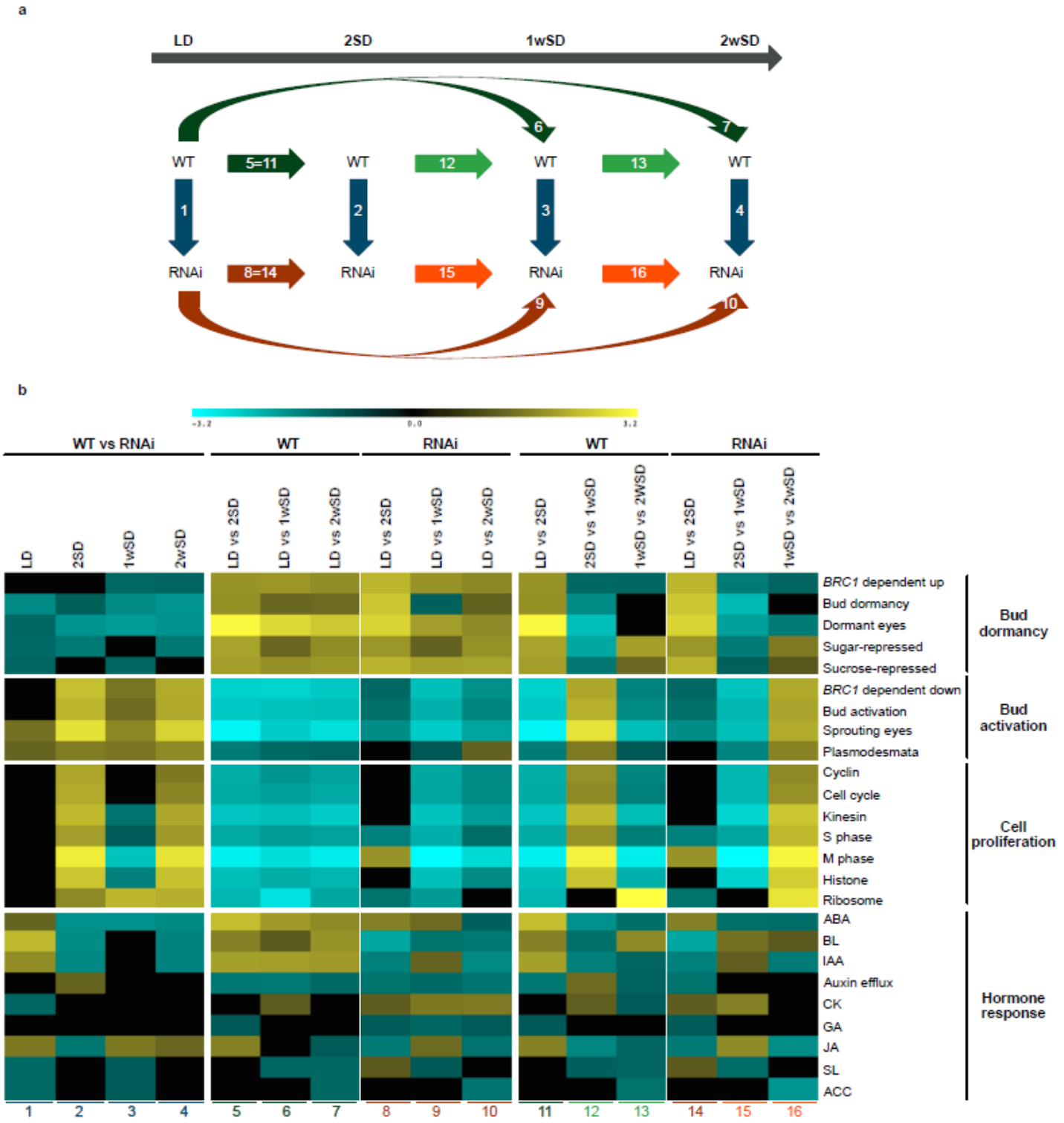

Figure 3

BRC1b RNAi buds remain active in SD. a, Experimental design of the RNA-seq time course. Comparisons performed are numbered and correspond to columns in (b). b, GSEA results for all samples and gene sets based on their normalized enrichment score (NES) for each sample. Complete results are in https://bioinfogp.cnb.csic.es/files/projects/nicolas_et_al_2020_gsea/. Positive NES values (yellow) indicate gene sets overrepresented among induced genes. Negative NES values (blue) indicate gene sets

overrepresented among repressed genes. Null values indicate gene sets not significantly overrepresented among either induced or repressed genes. Notice that 5=11 and 8=14. Gene sets are listed in Supplementary Table 3. ABA, abscisic acid; BL, brassinosteroid; IAA, Indole-3-acetic acid (auxin); CK, cytokinin; GA, gibberellic acid; JA, jasmonate; SL, strigolactone; ACC, 1-Aminocyclopropane-1-carboxylic acid (ethylene). Numbers under the columns refer to the comparisons depicted in a.

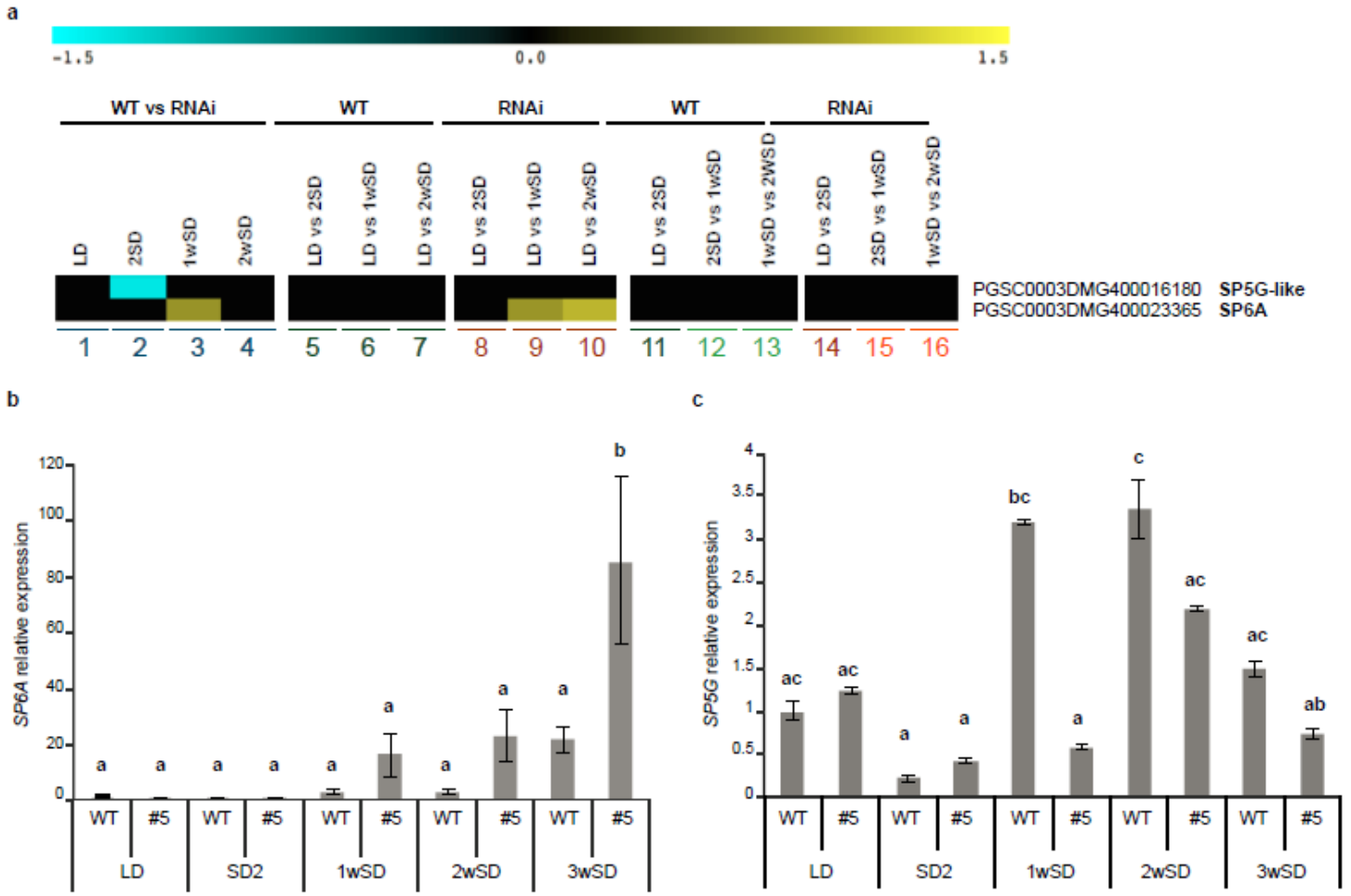

Figure 4

Expression of SP6A and SP5G in axillary buds during the time course. a, Heat map of SP6A and SP5G expression. Colors represent the log 2 fold change values. Column numbers correspond to comparisons performed as indicated in Fig. 3a. Positive values (yellow) indicate relative up-regulation and negative values (blue) relative down-regulation. mRNA levels of SP6A (b) and SP5G (c) during the time course, analysed by qPCR. WT and RNAi line #5 were analyzed in LD, and after two days (2SD), one week (1wSD), two weeks (2wSD) and three weeks (3wSD) in SD. Results are mean of three biological replicates. Error bars are SEM. Different letters above bars indicate significant differences among means (one-way ANOVA, $P < 0.05$).

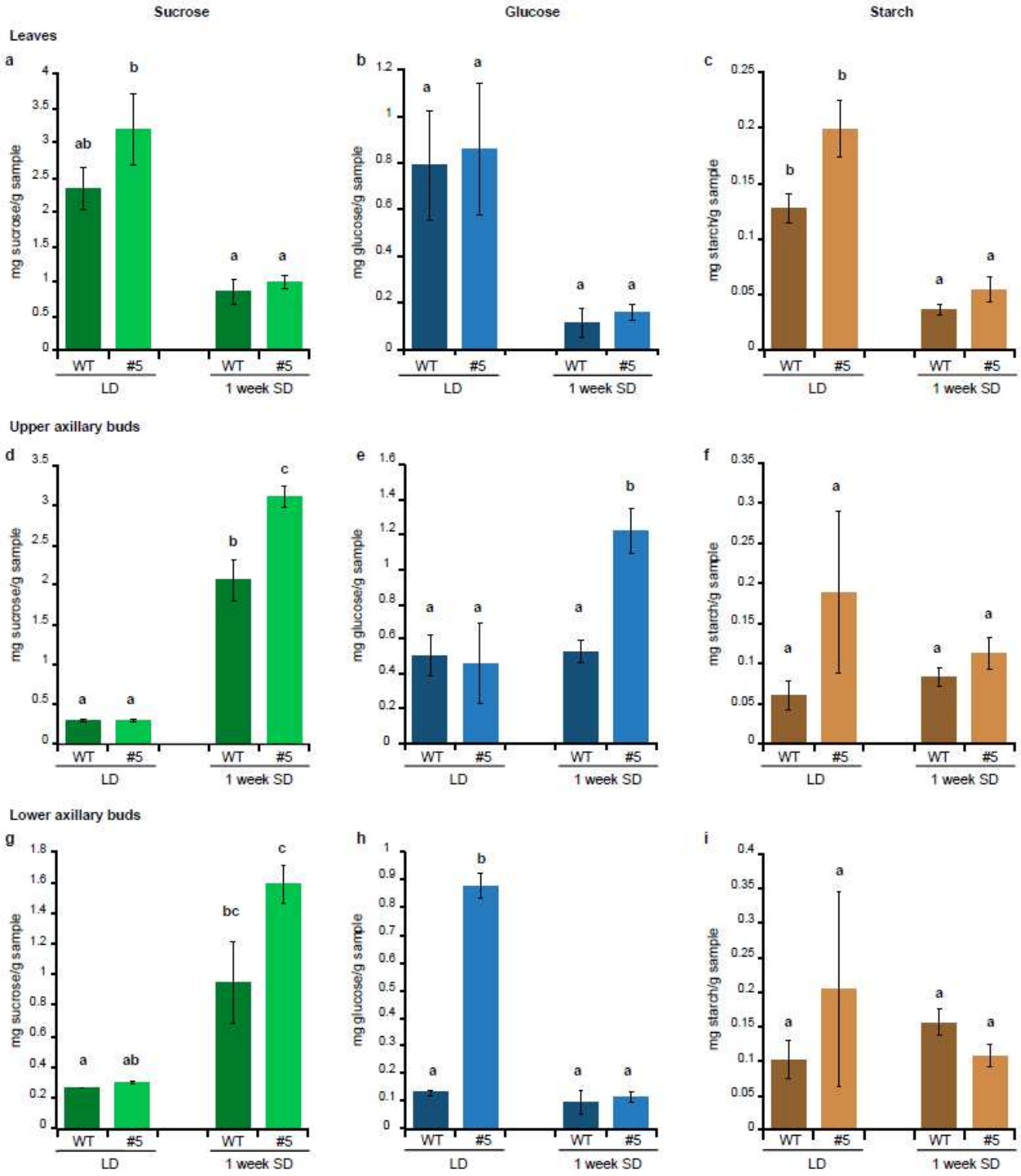

Figure 5

Carbohydrate content in WT and RNAi leaves and buds. Sucrose (a,d,g), glucose (b,e,h) and starch (c,f,i) quantification in leaves (a-c) axillary buds of upper nodes (d-f) and axillary buds of lower nodes (g-i). Sugar content was quantified in plant grown six weeks in LD, or five weeks in LD followed by one week in SD. Results are mean of three biological replicates. Error bars are SEM. Different letters above bars indicate significant differences among means (one-way ANOVA, $P < 0.05$).

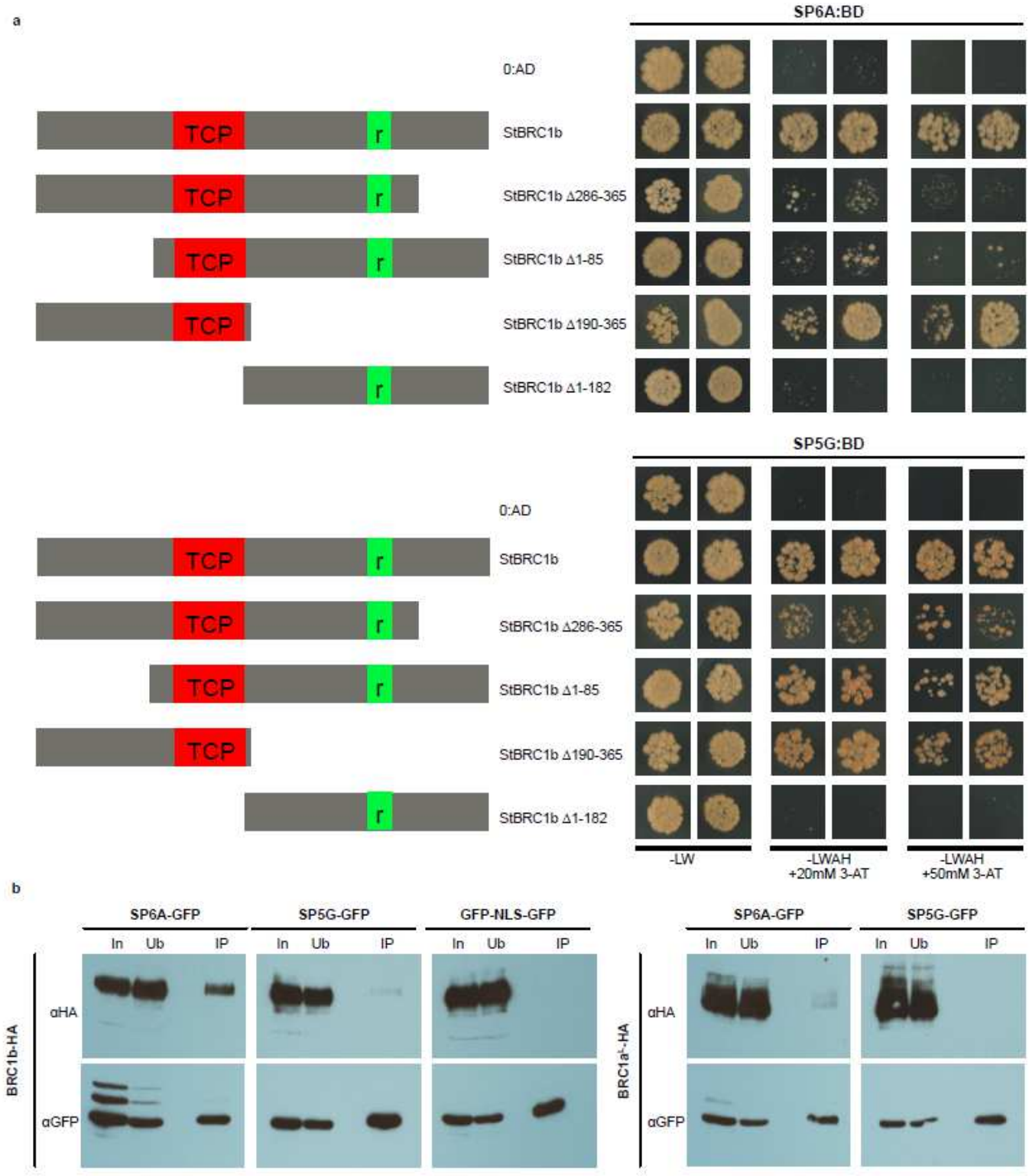

Figure 6

BRC1b interacts with SP6A in yeast and in planta. a, Yeast two-hybrid assays to test the interaction of BRC1b with SP5G and SP6A. SP5G and SP6A were fused to the GAL4 binding domain (BD) and used as baits. BRC1b and its truncated forms were fused to the GAL4 activation domain (AD). The empty vector pGADT7 (0:AD) was used as a negative control. –LW, medium lacking Leucine (L) and Tryptophan (W); LWAH, selective medium lacking Leucine (L) and Tryptophan (W), adenine (A) and Histidine (H); 3-AT, 3-

amino- 1,2,4-triazole. b, Co-immunoprecipitation assay. BRC1b:HA or BRC1a:HA were co-expressed with either SP5G:GFP or SP6A:GFP in Nicotiana benthamiana leaves. A GFP protein fused to the nuclear localisation signal c-myc (GFP-NLS) was used as control. In, input fraction; Ub, unbound fraction; IP, immunoprecipitation fraction.

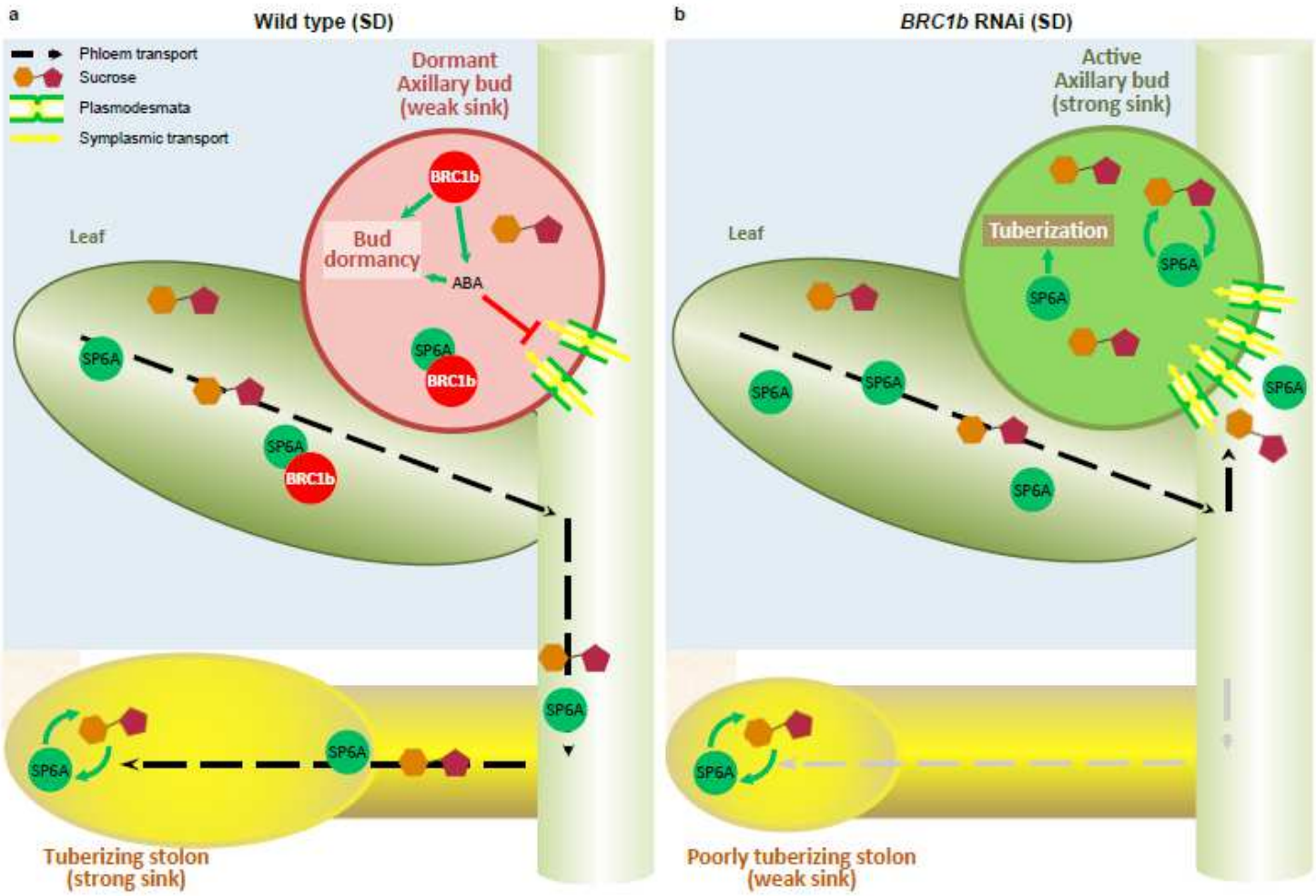

Figure 7

Model for the role of BRC1b in potato axillary buds. a, Under inductive conditions (SD), SP6A is induced in leaves and is phloem-transported along with sucrose. In WT, axillary buds accumulate BRC1b and become dormant, which renders the bud a weak sink. BRC1b enhances ABA signaling and downregulates plasmodesmata-related genes. This limits symplastic transport of sucrose and SP6A into the buds, which are instead preferentially transported basipetally to the stolons. In buds, free SP6A proteins are antagonized by direct interaction with BRC1b proteins. Green arrows indicate the positive feedback loop between sucrose and SP6A. b, In RNAi, lack of BRC1b leads to bud activation. ABA signaling is reduced, plasmodesmata genes are upregulated, and this facilitates import of sucrose and SP6A into the buds. Moreover, the SP6A proteins accumulated in buds are not blocked by BRC1b. Axillary buds become strong sinks that compete with stolons for sink dominance. This leads to alterations in the distribution of photoassimilates, which preferentially enter the aerial buds instead of being transported to stolons.

Supplementary Files

This is a list of supplementary files associated with this preprint. Click to download.

- SupplementaryFiguresoptimized.pdf
- SupplementaryTable1.pdf
- SupplementaryTable2Primerlist.xlsx
- SupplementaryTable3GSEALists.xlsx